Regenerative Therapy 26 (2024) 879–888

Contents lists available at ScienceDirect

Regenerative Therapy

journal homepage: http://www.elsevier.com/locate/reth

Original Article

The effects of local delivery of laurus nobilis extract and adipose derived stem cells via electrospun gelatin scaffold on spinal cord injury inflammatoradscy response and its regeneration

Chong Zhang [a], Jin Zhang [b], Daotao Xie [c, *], Gang Guo [c, **], Saman Jalili [d]

[a] Department of Rehabilitation Medicine, The First Affiliated Hospital of Guangzhou University of Chinese Medicine, Guangzhou, 510405, China
[b] Department of Emergency Traumatology, Gejiu People's Hospital, Yunnan, 661000, China
[c] Norxin International Science and Technology Base, Xi'an, 710032, China
[d] Department of Materials Science, Isfahan University of Technology, Isfahan, Iran

ARTICLE INFO

Article history:
Received 20 August 2024
Received in revised form
3 September 2024
Accepted 23 September 2024

Keywords:
Spinal cord injury
Drug delivery
Laurus nobilis extract
Electrospun scaffolds

ABSTRACT

When subjected to injury, the spinal cord's inherent complexity poses significant challenges for effective healing. In this study, gelatin nanofibers loaded with Laurus nobilis extract were developed to serve as a delivery system for adipose-derived stem cells (ADSCs), aiming to explore its potential immunomodulatory effects in a rat model of spinal cord injury. Through a series of in vitro assessments including scanning electron microscopy imaging, cell viability, anti-inflammatory, cell adhesion, biodegradation, and hemocompatibility assays, the characteristics of the delivery system were thoroughly evaluated. The in vitro studies revealed both the biocompatibility of the scaffolds and their notable anti-inflammatory properties, laying the groundwork for further investigation. Subsequent in vivo experiments demonstrated that rats treated with Laurus nobilis extract and ADSCs loaded scaffolds exhibited heightened functional recovery (BBB score of 14.66 ± 1.52 % and hot plate latency time of 8.33 0.26 s) and histological restoration at the 8-week mark post-injury. Notably, ELISA assay results revealed a significant reduction in tissue expression levels of key pro-inflammatory cytokines, including TNF-α, IL-1β, and IL-6, suggesting a pronounced immunomodulatory effect of the Laurus nobilis extract-loaded scaffolds. The findings underscore the potential of this novel delivery system to improve clinical outcomes in spinal cord injury by enhancing functional recovery and reducing inflammation. This approach could lead to the development of new, natural-based therapeutic strategies for spinal cord injury, with potential extensions to other inflammatory or degenerative conditions. Future research should focus on optimizing this strategy in larger animal models and eventually translating these findings into human clinical trials.

1. Introduction

The spinal cord, a vital component of the central nervous system, serves as a conduit for transmitting signals between the brain and the rest of the body. When subjected to injury, the spinal cord's inherent complexity poses significant challenges for effective healing [1,2]. Recent advances in scaffold technology have significantly improved tissue engineering and regenerative medicine. Innovations such as electrospinning have enabled the creation of nanofibrous scaffolds that closely mimic the extracellular matrix, enhancing cell attachment and tissue integration. Additionally, 3D printing has allowed for the fabrication of complex scaffold structures with precise control over pore size and mechanical properties [3,4]. In drug delivery, advancements in controlled-release systems and targeted delivery techniques have enhanced the efficacy of therapeutic agents [5].

Notably, the inflammatory response triggered by spinal cord injury (SCI) can exacerbate tissue damage, creating a hostile microenvironment that impedes regenerative processes. To address this intricate challenge, researchers have turned their attention to the potential therapeutic benefits of immunomodulatory agents [6]. In this context, Laurus nobilis, commonly known as bay laurel, has been a subject of interest in traditional medicine for its diverse pharmacological properties. Recent studies have highlighted its potential to modulate inflammatory responses and promote tissue

* Corresponding author.
** Corresponding author.
E-mail addresses: daotaoxie@sina.com (D. Xie), gang.guo@norxin.com (G. Guo).
Peer review under responsibility of the Japanese Society for Regenerative Medicine.

https://doi.org/10.1016/j.reth.2024.09.008

regeneration [7]. In the context of SCI, the inclusion of Laurus nobilis extract in the therapeutic arsenal introduces a botanical dimension to the conventional approaches, offering a natural and complementary avenue for intervention.

Complementing the anti-inflammatory properties of Laurus nobilis extract (LNE), adipose-derived stem cells (ADSCs) bring a regenerative prowess to the therapeutic landscape. ADSCs are mesenchymal stem cells sourced from adipose tissue, possessing the ability to differentiate into various cell types and promote tissue repair [8,9]. Studies in animal models have demonstrated that ADSCs can promote functional recovery and reduce spinal cord damage when transplanted, leading to improved hindlimb motor function and reduced cavitation at the injury site. These beneficial effects are attributed to multiple mechanisms, including the secretion of growth factors and cytokines, activation of neuroprotective signaling pathways, and promotion of angiogenesis [10,11]. ADSCs offer several advantages over other stem cell types, such as easier accessibility, lower tumorigenicity risk, and fewer ethical concerns. While primarily still in the research stage, early clinical trials have suggested that ADSC transplantation is safe for SCI patients, with some therapeutic effects observed in human studies [12].

The delivery method is equally pivotal in ensuring the effective deployment of therapeutic agents within the SCI site. In this study, we leverage the versatility of electrospun gelatin scaffolds as a vehicle for local drug delivery. Electrospinning, a technique that produces nanofibrous structures resembling the extracellular matrix (ECM), provides a biomimetic platform for cell attachment, proliferation, and controlled release of therapeutic agents [13,14]. The electrospun gelatin scaffold serves as a three-dimensional support structure, facilitating the sustained and targeted delivery of both LNE and ADSCs to the injured spinal cord. In the context of cell delivery via electrospun scaffolds, Liu et al. demonstrated that induced neural stem cells seeded on PLGA-PEG scaffolds survived, self-renewed, and differentiated into neurons and glial cells. The scaffolds restored spinal cord continuity, reduced cavity formation, and improved functional recovery in a rat spinal cord injury model, highlighting their potential as a promising treatment for spinal cord repair [15]. Xu et al. developed collagen-based fiber bundles using electrospinning techniques to enhance stem cell transplantation in spinal cord injury. In vivo results showed the fibers promoted anti-inflammatory effects, released brain-derived neurotrophic factor, and supported stem cell differentiation into neurons, leading to improved neurological recovery and function [16].

The objective of this study is to investigate the therapeutic potential of combining LNE with ADSCs delivered via electrospun gelatin scaffolds to promote tissue repair in a rat model of SCI. This approach represents a novel strategy compared to existing methods by leveraging the anti-inflammatory properties of LNE and the regenerative capabilities of ADSCs, delivered through a scaffold that mimics the extracellular matrix, enabling localized and sustained release of therapeutic agents. By targeting both inflammation and tissue regeneration, this dual-action therapy aims to overcome current limitations in SCI treatment, offering a more effective and minimally invasive option for enhancing healing and functional recovery.

2. Methods and materials

2.1. Preparation of LNE-loaded gelatin nanofibers

Initially, Gelatin (Type A, Sigma Aldrich) was dissolved in acetic acid (Glacial, Merck) to achieve a final concentration of 28 wt%. Once a clear solution was obtained, 1 ml of LNE extract (Ethanolic, obtained from Barij, Iran) was thoroughly mixed with 9 ml of the gelatin solution. Subsequently, the LNE-gelatin solution was loaded into a 10 ml syringe connected to an 18-gauge metal needle. Employing a positive high voltage at a magnitude of 18 kV, the polymeric solution underwent electrospinning. The polymer feeding rate was maintained at 0.7–1 ml/h, the needle-to-collector distance was set at 15–17 cm, and the mandrel's turning rate was adjusted to 500–600 rpm. After the production of scaffolds, they were cross-linked in glutaraldehyde vapor for 1 h and rinsed three times in distilled water.

2.2. Scanning electron microscopy assay

LNE-gelatin scaffolds and scaffolds lacking LNE underwent a gold coating process lasting 250 s before being subjected to SEM imaging at an accelerating voltage of 25 kV.

2.3. Cell viability assay

The viability of ADSCs (Pasteur Institute, Iran) cultured on LNE-gelatin and gelatin scaffolds was assessed using Alamar blue assay (Invitrogen, USA). Briefly, scaffolds were sterilized using 70 % ethanol for 30 min and 15 min UV radiation (Each side). Then, ADSCs were seeded onto the scaffolds at 10,000 cells per cm2 in 50 μl culture media and cultured for 7 days. On days, 2, 4, and 7, 1 ml of Alamar blue solution was mixed with 9 ml of complete culture media and 300 μl of this solution was poured onto the samples and incubated for 3 h. Finally, the absorbance of samples was read at 570 nm.

2.4. Cell viability assay under oxidative stress

The viability of ADSCs cultured on LNE-gelatin and gelatin scaffolds under H2O2-induced oxidative stress was assessed using Alamar blue assay (Invitrogen, USA). Briefly, scaffolds were sterilized using 70 % ethanol for 30 min and 15 min UV radiation (Each side). Then, ADSCs were seeded onto the scaffolds at 10,000 cells per cm^2 in 50 μl culture media and cultured for 48 h. Then, 1 % H2O2 solution was added into each well and cells were incubated for 1 h. Finally, cell viability assay was performed as described in section 2-3.

2.5. Anti-inflammatory assay

The evaluation of the anti-inflammatory potential of RAW 264.7 macrophage cells was conducted through an ELISA assay. In a nutshell, scaffolds underwent sterilization using 70 % ethanol for 30 min and received 15 min of UV radiation on each side. Following sterilization, macrophages were seeded onto the scaffolds at a density of 40,000 cells per cm^2 in 50 μl of culture media and were cultured for 36 h. Subsequently, each well received a supplementation of 1 μg/ml LPS (Sigma), and the cells were incubated for an additional 12 h. The quantification of pro-inflammatory cytokines, including IL-6 and IL-1β, was carried out using ELISA Assay kits sourced from Abcam, USA.

2.6. DPPH assay

The radical scavenging ability of LNE-gelatin and gelatin scaffolds was evaluated through the implementation of a DPPH assay. Specifically, segments of pure gelatin scaffolds and gelatin scaffolds incorporating LNE were cut into dimensions of 10×10 cm^2. Then, they were immersed in liquid nitrogen and

ground into fine powders. Subsequently, various concentrations of these samples were immersed in 3 ml of a 0.1 mM DPPH solution dissolved in methanol, allowing for interaction over a 9-h period at room temperature.

In this experimental setup, ascorbic acid was employed as the standard control, while DPPH-only samples functioned as the negative control group. To quantify the percentage of DPPH radical scavenging, a spectrophotometric method at 517 nm was utilized. The radical scavenging activity was determined using the formula:

Radical scavenging activity (%) = (Absorbance of Control-Absorbance of control / Absorbance of sample) × 100

2.7. Mechanical strength analysis

The ultimate tensile strength of both gelatin and LNE-gelatin scaffolds was determined using a uniaxial tensile testing device (Santam, Karaj, Iran) with an extension rate set at 1 mm/min, following a methodology inspired by the approach utilized in measuring the tensile strength of manufactured scaffolds. The scaffolds, cut in standardized dimensions, were securely attached to the grips of the testing apparatus. The testing device was configured to apply a uniaxial tensile force at a consistent rate of 1 mm/min until the samples failure.

2.8. Cell adhesion studies

The adhesion of ADSCs cultured on LNE-gelatin and gelatin scaffolds was assessed using DAPI staining. Briefly, cells were cultured onto the scaffolds at the density of 40,000 cells/cm^2 and cultured for 48 h. Then, the cells were incubated with DAPI dye (Invitrogen, USA) for 15 min and then imaged under fluorescent microscope.

2.9. Hemocompatiblity assay

The hemolysis assay for LNE-gelatin and gelatin scaffolds was carried out using rat whole blood that was anticoagulated and subsequently diluted with normal saline. The samples underwent incubation with 200 μl of the blood samples at 37 °C for 60 min, followed by centrifugation at 1500 rpm for 10 min. The resulting supernatant was then analyzed for absorbance at 545 nm using a Multi-Mode Microplate Reader (BioTek Synergy 2). In this assay, the negative control consisted of whole blood diluted in normal saline, while the positive control involved whole blood diluted in deionized water.

2.10. Release assay

Release of LNE from the matrix of electrospun gelatin scaffolds was assessed using UV–visible spectroscopy method. Briefly, 200 mg of LNE-gelatin scaffolds was immersed in 10 ml of PBS and kept at 37 °C for 3 days. On different time points, 0.5–0.6 ml of the release media was taken and its absorbance was read at 361 nm. The acquired measurements were fitted into the standard curve of LNE in PBS and the amount of release LNE was calculated. Finally, cumulative drug release was reported.

2.11. Preparation of ADSCs-seeded constructs for implantation

LNE-gelatin and gelatin scaffolds were sterilized and seeded with ADSCs at the density of 40,000 cells per cm^2 and cultured for 48 h with DMEM-F12 (Invitrogen, USA) containing 10 % FBS (Gibco, USA) and 1 % antiobiotics (Gibco, USA). Then, the scaffolds were taken and implanted at the injury site.

2.12. In vivo study

2.12.1. Surgery procedure

In vivo studies This project was approved by the Ethics Review Committee of Guangzhou Ruiye Model Animal Center (Approval No. A202312525). Fifteen male Wistar rats were randomly divided into three groups as follows:1- LNE-gelatin-ADSCs, 2- gelatin-ADSCs, and negative control (in which the animals received no treatment following injury). The animals were then anesthetized via intraperitoneal injection of ketamine and xylazine (100 mg/kg and 10 mg/kg, respectively). Subsequently, the dorsal skin was trimmed, and the surgery region was disinfected using ethanol and povidone iodine. A surgical incision was then executed along the vertebral column, revealing the vertebrae. T-9 laminectomy was performed, involving the incision of the dura matter and the execution of T9 dorsal hemisection. Then LNE-gelatin-ADSCs and gelatin-ADSCs were implanted at the injury site and fixed in place by suturing. The dura matter, skin, and muscle tissues were subsequently stitched, concluding with the closure of the injury site. The animals were kept for the total duration of 8 weeks. The choice of the Wistar rat model for this study is well-justified due to its established relevance to human SCI research. Wistar rats are frequently used in preclinical studies because their spinal cord anatomy and injury responses closely mimic those of humans, allowing for reliable evaluation of therapeutic interventions.

2.12.2. Behavior factors assessment

The assessment of motor function recovery post hydrogel injection was conducted on weeks 4 and 8 using the Basso, Beattie, and Bresnahan (BBB) experiment, as detailed in a prior study [17]. Two impartial observers, unaware of the experimental conditions, examined hind limb movements. In addition, we examined the restoration of sensory function during the fourth and eighth weeks through the Hot Plate Latency (HPL) test. In essence, members of each group were positioned on a hot plate set at 56 °C, and the duration until the animals exhibited a reaction was recorded. A cut-off time of 12 s was established for this experiment.

2.12.3. ELISA assay

On week 8 following the surgery, the animals were sacrificed and their spinal cord tissues were harvested for assessing the tissue expression levels of IL-6, IL-1β, and TNF-α using ELISA assay kits (Abcam, USA).

2.12.4. Histopathological examinations

On week 8th, the animals were sacrificed and the spinal cord tissue at the injury site was assessed for histopathological examinations using Hematoxylin and Eosine (H&E) and Luxal fast blue staining.

2.12.5. Histomorphometry analysis

Volume measurements were acquired through the Cavalieri method employing computer-assisted microscopy. Calculation involved the total volume of intact white matter, unaffected gray matter, lesion volume, and overall cord volume. An observer manually delineated contours using the 4 × objective, and the 20 × objective aided in defining tissue boundaries. A point-grid with known spacing was randomly superimposed on the live section image, and points within the region of interest were tallied. Subsequently, volume was assessed using the ensuing formula:

$$V = \sum F \times \text{Area} \times \text{Distance}$$

where, "V" is the total volume, "∑F" is the total number of points hitting region of interest, "Area" is the area associated with each point.

The ultimate post-processing thickness of sections, gauged with the microcator, was applied in the computation of distance. Lesion length was ascertained by determining the distance between the sections at the most rostral and caudal points where no visible lesion or abnormal tissue architecture was observed.

2.13. Statistical analysis

Data was analyzed using Graph pad prism via student's t-test and one-way ANOVA tests. All experiments were repeated at least three times.

3. Results

3.1. SEM imaging results

The outcomes presented in Fig. 1 indicate that both LNE-gelatin and gelatin scaffolds exhibited a web-like structure characterized by fibers arranged in a random orientation. The integrity of the fibers was effectively maintained, and there were no observable signs of disintegration. The average fiber size of LNE-gelatin and gelatin was measured to be around 599.77 ± 205.46 nm and 601.72 ± 211.02 nm, respectively.

3.2. Cell viability assay

Results (Fig. 2 A) showed that at none of the studied time points, LNE-gelatin and gelatin scaffolds did not impart significant toxicity towards ADSCs. However, under oxidative stress gelatin and control group had significantly lower cell viability than LNE-gelatin group (Fig. 2 B), indicating that LNE has protected ADSCs against oxidative stress.

3.3. Anti-inflammatory assay results

Results (Fig. 3 A) showed that macrophages cultured on LNE-gelatin and gelatin scaffolds released significantly lower amounts of IL-6 and IL-1β compared with the cells cultured on tissue culture plate or gelatin scaffolds.

3.4. DPPH assay results

Results (Fig. 3 B) showed that ascorbic acid had the highest potential for quenching DPPH free radicals. In addition, LNE-gelatin group had higher radical scavenging activity than gelatin-only group. Therefore, incorporation of LNE into the scaffolds has augmented their ability to quench free radicals.

3.5. Mechanical strength analysis results

Results showed that LNE-gelatin and gelatin scaffolds had around 1.25 0.36 ± MPa and 1.43 ± 0.07 MPa ultimate tensile strength, respectively.

3.6. Cell adhesion studies

Results (Fig. 4) showed that ADSCs adhered to the surface of both LNE-gelatin and gelatin scaffolds and populated their surface.

3.7. Hemocompatibility assay

Results (Fig. 5) showed that none of the LNE-gelatin and gelatin scaffolds imparted significant hemolysis compared with the normal saline group. Positive control group had significantly higher hemolysis activity than other groups.

3.8. Release assay results

Results (Fig. 3C) showed that LNE was released from the matrix of LNE-gelatin scaffolds in a sustained manner. The cumulative release gradually increased and reached to almost 100 % at the end of 3rd day post-immersion in PBS.

3.9. In vivo study results

3.9.1. Behavioral factors assessment

Results (Fig. 6 A) showed that on week 4 and 8 LNE-gelatin-ADSCs group had significantly higher BBB scores than the negative control group. On week 8, LNE-gelatin-ADSCs group had significantly higher BBB score than gelatin-ADSCs group. At the same time point, gelatin-ADSCs group had significantly higher BBB score than the negative control group. Hot plate latency test results (Fig. 6 B) showed that on week 8th, LNE-gelatin-ADSCs group had significantly faster response time than negative control and gelatin-ADSCs groups.

3.9.2. Histological evaluation results

H&E staining images (Fig. 7) revealed that the LNE-gelatin-ADSCs group exhibited distinct gray and white matter regions, indicating robust cellular and structural regeneration. The well-defined boundaries pointed towards a significant restoration process. The heightened neuronal density observed in this group provided further evidence of cellular proliferation and maturation, suggesting the potential for functional recovery. Conversely,

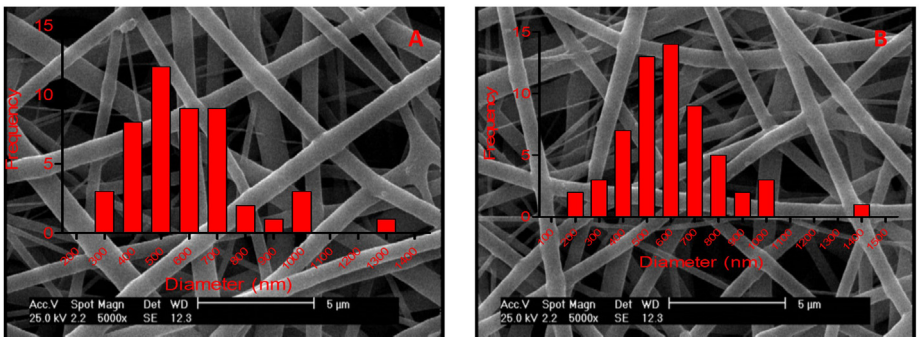

Fig. 1. Representative SEM images of (A) LNE-gelatin and (B) gelatin scaffolds.

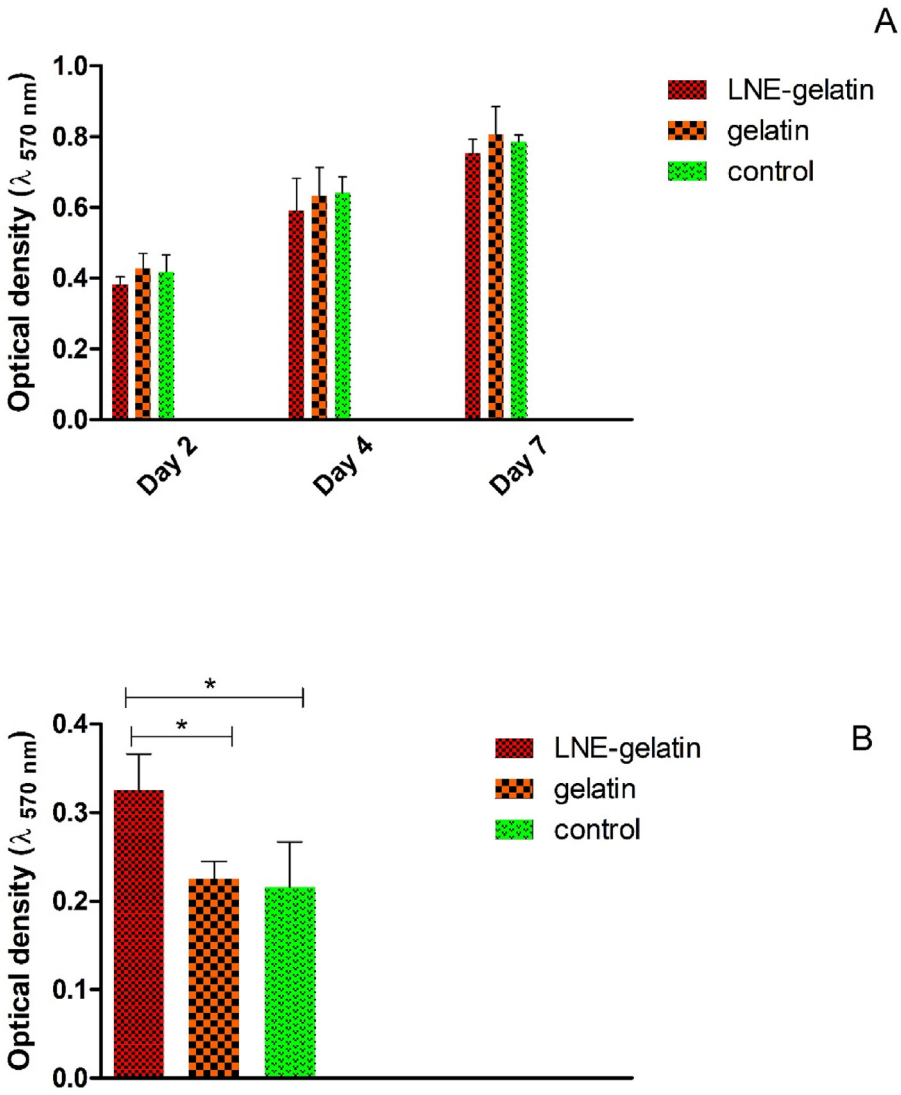

Fig. 2. MTT assay under normal (A) and (B) oxidative stress conditions with ADSCs cultured on LNE-gelatin scaffolds compared with the cells cultured on tissue culture plate, * shows p-value <0.05.

animals treated with gelatin-ADSCs displayed signs of vacuolation and edema. Moreover, there was a noticeable increase in the infiltration of pro-inflammatory cells in this group compared to the LNE-gelatin-ADSCs group. The negative control group exhibited the most unfavorable tissue repair responses, as evidenced by pronounced edema and vacuolation, accompanied by an exacerbated inflammatory reaction.

Luxol fast blue staining outcomes (Fig. 8) indicated abundant blue staining in spinal cord injuries treated with LNE-gelatin-ADSCs, indicating the existence of well-structured myelin sheath. This suggests improved myelination and potential neuroprotective effects. In this particular group, a substantial amount of nerve myelin was observed around the implant site, whereas the other three groups exhibited significantly lower myelin density and positive area.

3.9.3. Histomorphometry analysis

Results (Fig. 9) showed that lesion volume and lesion length in the LNE-gelatin-ADSCs group were significantly lower than gelatin-ADSCs and negative control group. In addition, these parameters in the gelatin-ADSCs group were significantly lower than the negative control groups. Preserved gray and white matter volume in the LNE-gelatin-ADSCs group were significantly higher than gelatin-ADSCs and negative control groups. These parameters in the gelatin-ADSCs group were significantly higher than the negative control group.

3.9.4. ELISA assay results

Results (Fig. 10) showed that the tissue concentrations of IL-6, TNF-α, and IL-1β in spinal cord tissues treated with LNE-gelatin-ADSCs group were significantly lower than the tissues in the gelatin-ADSCs and negative control groups. These cytokines levels in the gelatin-ADSCs group were significantly lower than the negative control group.

4. Discussion

The versatile capability of electrospun scaffolds for cell and drug delivery enhances their therapeutic potential in treating SCI [18,19]. These nanofibrous matrices emulate the ECM, offering structural support and facilitating cell attachment, proliferation, and differentiation. Loaded with therapeutic agents, they foster a conducive

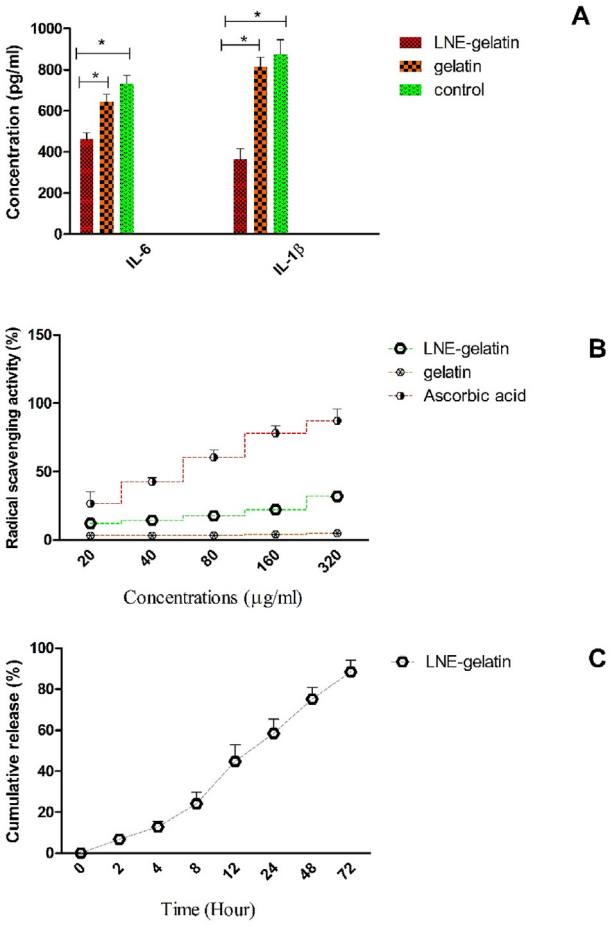

Fig. 3. (A) Shows the anti-inflammatory activity of LNE-gelatin and gelatin scaffolds as compared with the macrophage cells cultured on the tissue culture plate and (B) shows the radical scavenging function of LNE-gelatin and gelatin scaffolds as compared to ascorbic acid as the standard control, and (C) shows release of LNE from the matrix of LNE-gelatin scaffolds, * shows p-value <0.05.

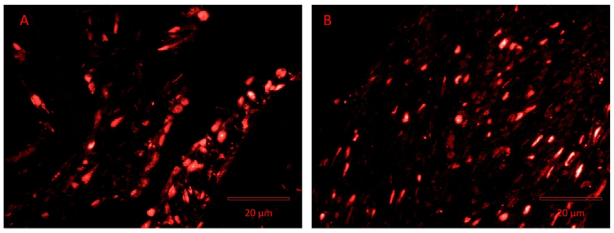

Fig. 4. Adhesion of ADSCs on (A) LNE-gelatin and (B) gelatin scaffolds.

microenvironment for tissue regeneration. In the current research, a nanofibrous delivery system was developed for sustained delivery of LNE and ADSCs for treating SCI in a rat model. Our microstructural analysis results confirmed the ECM-like architecture of the delivery system. It has been shown that such constructs are conductive for the adhesion and proliferation of various cell types [20]. Cell viability assay was performed in both normal and oxidative stress conditions. In accordance with the results of previous findings, our results validated the biocompatibility of electrospun gelatin scaffolds [21]. Under oxidative stress conditions, LNE-gelatin scaffolds significantly protected ADSCs against detrimental effects of oxidation. It could be that various polyphenolic compounds in LNE such as caffeic acid, apigenin, quercetin,

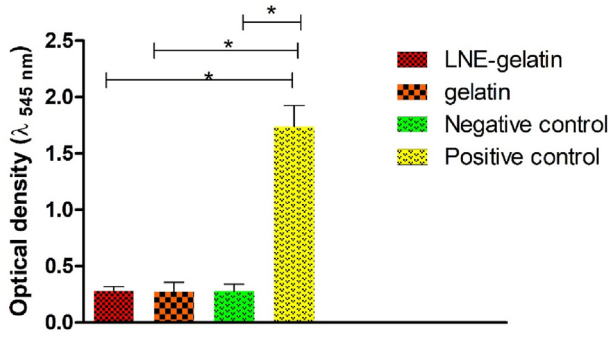

Fig. 5. Hemocompatiblity assay with LNE-gelatin and gelatin scaffolds compared with normal saline and distilled water as negative and positive control groups, respectively.

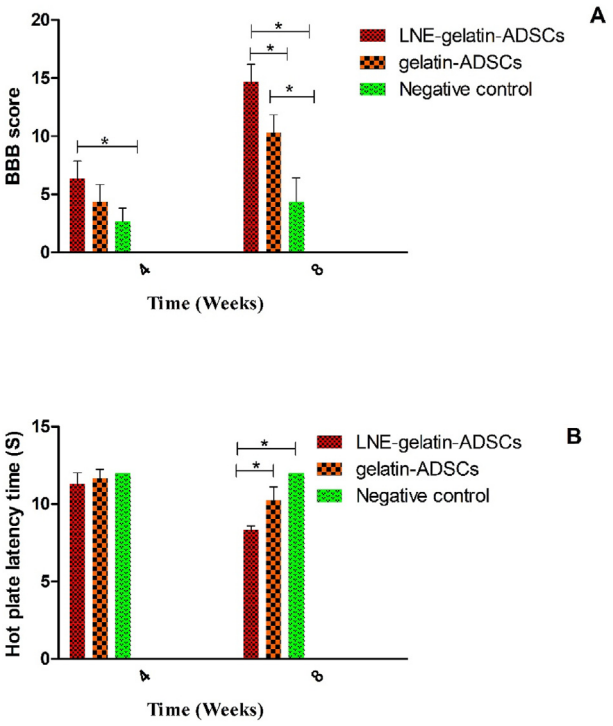

Fig. 6. Histograms showing (A) BBB scores and (B) hot plate latency test results in animals treated with LNE-gelatin-ADSCs and gelatin-ADSCs groups on weeks 4 and 8 after injury, * shows p-value <0.05.

epicatechin, and kaempferol have quenched H_2O_2 free radicals and improved cells viability [22]. This theory is in accordance with the results of DPPH assay that showed higher radical scavenging function of LNE-gelatin scaffolds. LNE demonstrates the ability to eliminate hydroxyl radicals, which play a significant role in inducing molecular and cellular harm within living organisms [23]. Anti-inflammatory assay showed that LNE's incorporation augmented immunomodulatory function of gelatin scaffolds. Studies have shown that the LNE has the ability to manage inflammation by reducing the activation of NLRP3 inflammasome. This process works by preventing the activation of caspase-1, secretion of interleukin-1β, and the formation of ADSC pyroptosome complex [24]. High mechanical strength of drug delivery systems guarantees their easy application during implantation. Our developed delivery systems tensile strength could be explained by the entanglement of gelatin nanofibers in different directions (as observed in SEM images). Adhesion of ADSCs to the surface of our

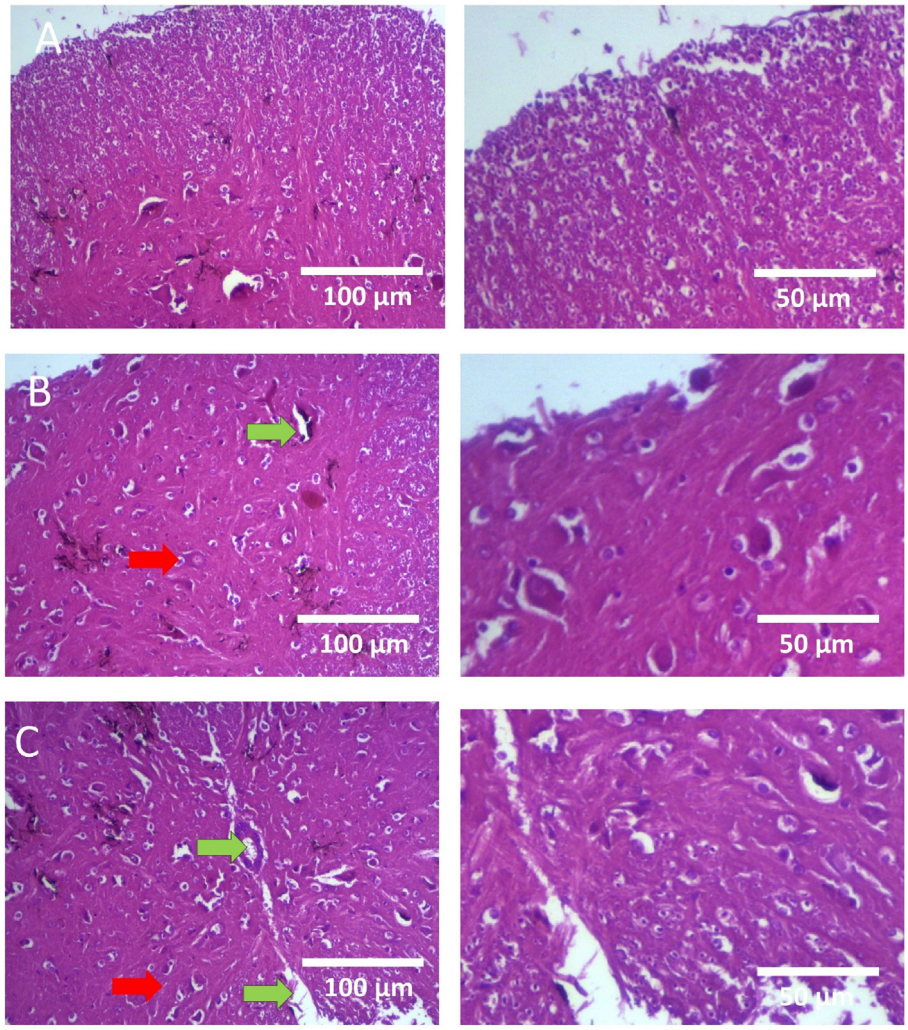

Fig. 7. H&E staining images of spinal cord tissues in (A) LNE-gelatin-ADSCs group, (B) gelatin-ADSCs group, and (C) negative control group. Green arrows show vacuolation and red arrow show edema.

scaffolds could be explained by the fact that cells adhere to gelatin scaffolds primarily through integrin-mediated binding. Integrins are cell surface receptors that interact with specific ligands, such as proteins within the gelatin matrix, facilitating attachment and subsequent signaling for cell proliferation and differentiation [25,26]. In accordance with the results of previous findings, we showed hemocompatibility of the electrospun scaffolds. Release assay results showed that LNE was released from the matrix of gelatin scaffolds in a sustained manner. This result could be attributed to the diffusion, swelling, or gradual erosion of gelatin in contact with aqueous solutions. However, combinations of these mechanisms may occur in the in vivo settings [27]. In vivo results showed that local delivery of LNE and ADSCs significantly augmented functional recovery after SCI. Local delivery of these compounds serves multiple functions in the context of SCI repair. LNE's bioactive components, such as flavonoids and essential oils, exhibit antioxidative and anti-inflammatory effects, which can mitigate secondary damage following injury [28,29]. Lee et al. showed that LNE inhibited NLRP3 inflammasome activation in mouse macrophages, reducing caspase-1 activation, interleukin-1β secretion, and proinflammatory cytokines. The major component, 1,8-cineole, consistently suppressed inflammasome activation, revealing its anti-inflammatory mechanism [24]. Additionally, flavonoid compounds within the extract may promote neuronal survival and axonal regeneration [30]. By delivering the extract directly to the injury site, its therapeutic effects are maximized, potentially enhancing tissue repair. Combining LNE with ADSCs capitalizes on the synergistic effects of both modalities. ADSCs possess the ability to differentiate into various cell types, including neurons and glial cells, contributing to tissue regeneration. Moreover, they secrete trophic factors that support neuronal survival, angiogenesis, and immunomodulation [31,32]. When administered alongside LNE, ADSCs may enhance its neuroprotective and anti-inflammatory effects while promoting tissue regeneration through paracrine signaling mechanisms. The observed reduction in tissue expression levels of pro-inflammatory cytokines (as shown in ELISA assay results) further underscores the therapeutic potential of this combined approach. IL-6, IL-1β, and TNF-α are key mediators of inflammation and secondary tissue damage following SCI [33,34]. By attenuating their expression, LNE and ADSCs create a more favorable microenvironment for tissue repair, potentially facilitating functional recovery. In accordance with our results, Ryu et al. evaluated the effect of allogenic ADSCs on neurological function in a canine SCI model. ADSCs significantly improved pelvic limb function, nerve conduction velocity, and histological markers compared to control and vehicle groups [35]. Silva et al. developed

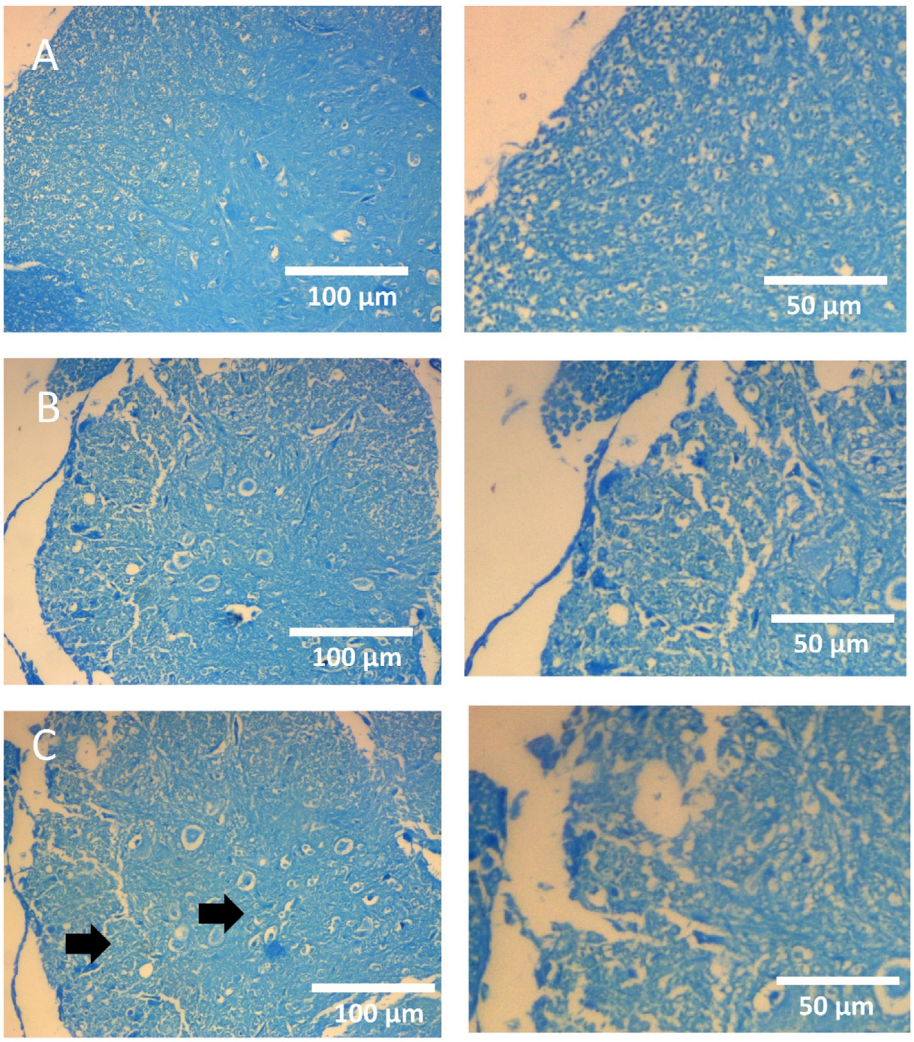

Fig. 8. Luxol fast blue staining images of spinal cord tissues in (A) LNE-gelatin-ADSCs group, (B) gelatin-ADSCs group, and (C) negative control group. Black arrow shows axonal disintegration.

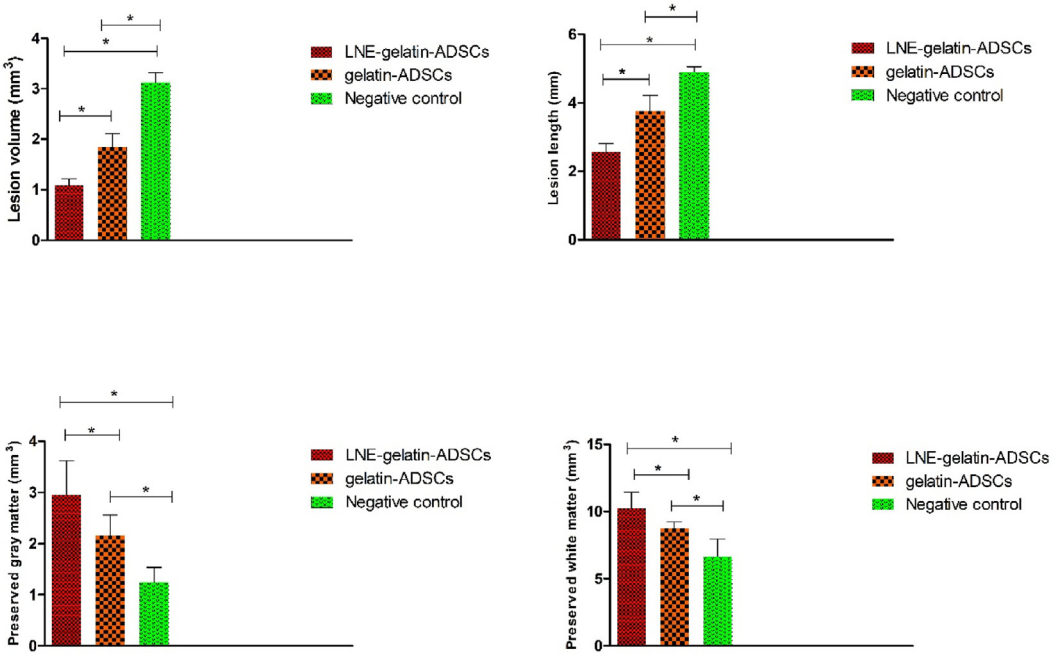

Fig. 9. Histomorphometry analysis in spinal cord tissues stained with H&E at the end of 8th week after the injury. * Shows p-value <0.05.

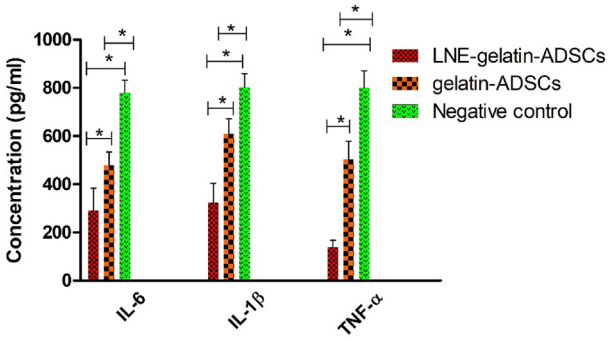

Fig. 10. ELISA assay results in spinal cord tissues treated with different treatment strategies, * shows p-value <0.05.

a hydrogel delivery system for human ADSC secretome, composed of star-shaped poly (ethylene glycol) (starPEG) and heparin, designed to release pro-regenerative mediators like IL-4, IL-6, and neurotrophic factors over 10 days. The system enhanced neural differentiation, neurite growth, and motor function recovery in spinal cord injury models by reducing microglial activation and increasing anti-inflammatory cytokines [36]. This approach could enhance therapeutic outcomes by addressing both inflammation and tissue repair. This novel combination therapy could potentially improve motor function, reduce complications, and offer a more effective alternative to existing treatments, thereby advancing the clinical management of SCI.

5. Conclusion

In conclusion, our study represents a significant advancement in the pursuit of effective treatments for spinal cord injury, a condition characterized by its formidable challenges to healing. By developing gelatin nanofibers loaded with laurus nobilis extract as a delivery system for adipose-derived stem cells (ADSCs), we aimed to address the complex immunomodulatory needs of spinal cord injury repair. Through meticulous in vitro evaluations encompassing various parameters, we laid a robust foundation for subsequent investigations. The promising outcomes of our in vivo experiments, showcasing improved functional recovery and histological restoration in rats treated with the novel delivery system, underscore its therapeutic potential. Particularly noteworthy is the significant reduction in tissue expression levels of key pro-inflammatory cytokines, indicative of the pronounced immunomodulatory effects conferred by our scaffolds. To further validate and expand on our findings, future experiments could involve testing alternative scaffold materials, such as polyurethane or silk fibroin, and exploring combinations of LNE with other therapeutic agents to assess their synergistic effects on neural regeneration. Long-term studies in rat models are needed to evaluate the durability and sustained effectiveness of the treatments, along with mechanistic studies to understand the underlying biological processes. For clinical translation, comprehensive pre-clinical safety and efficacy studies should precede Phase I trials to assess the safety and tolerability of the scaffold-based therapy. Successful Phase I trials would lead to Phase II and III trials to test effectiveness in larger patient groups, followed by regulatory approvals. This research significantly advances the field by providing a novel dual-action approach to SCI treatment, potentially improving outcomes and offering more effective interventions compared to existing methods.

Funding

The authors declare that no funds, grants, or other support were received during the preparation of this manuscript.

Declaration of competing interest

The authors declare that they have no known competing financial interests or personal relationships that could have appeared to influence the work reported in this paper.

References

[1] Wang TY, Park C, Zhang H, Rahimpour S, Murphy KR, Goodwin CR, et al. Management of acute traumatic spinal cord injury: a review of the literature. Frontiers in surgery 2021;8:698736.
[2] Eli I, Lerner DP, Ghogawala Z. Acute traumatic spinal cord injury. Neurol Clin 2021;39(2):471–88.
[3] Pourkhodadad S, Hosseinkazemi H, Bonakdar S, Nekounam H. Biomimetic engineered approaches for neural tissue engineering: spinal cord injury. J Biomed Mater Res B Appl Biomater 2023;111(3):701–16.
[4] Hey G, Willman M, Patel A, Goutnik M, Willman J, Lucke-Wold B. Stem cell scaffolds for the treatment of spinal cord injury—a review. Biomechanics 2023;3(3):322–42.
[5] Gong W, Zhang T, Che M, Wang Y, He C, Liu L, et al. Recent advances in nanomaterials for the treatment of spinal cord injury. Materials Today Bio 2023;18:100524.
[6] Walsh CM, Gull K, Dooley D. Motor rehabilitation as a therapeutic tool for spinal cord injury: new perspectives in immunomodulation. Cytokine Growth Factor Rev 2023;69:80–9.
[7] Al-Mijalli SH, Mrabti HN, Ouassou H, Flouchi R, Abdallah EM, Sheikh RA, et al. Chemical composition, antioxidant, anti-diabetic, anti-acetylcholinesterase, anti-inflammatory, and antimicrobial properties of arbutus unedo L. And laurus nobilis L. Essential oils. Life 2022;12(11):1876.
[8] Zhang J, Liu Y, Chen Y, Yuan L, Liu H, Wang J, et al. Adipose-derived stem cells: current applications and future directions in the regeneration of multiple tissues. Stem Cell Int 2020:2020.
[9] Rafiei Alavi SN, Madani Neishaboori A, Hossein H, Sarveazad A, Yousefifard M. Efficacy of adipose tissue-derived stem cells in locomotion recovery after spinal cord injury: a systematic review and meta-analysis on animal studies. Syst Rev 2021;10:1–12.
[10] Ohta Y, Hamaguchi A, Ootaki M, Watanabe M, Takeba Y, Iiri T, et al. Intravenous infusion of adipose-derived stem/stromal cells improves functional recovery of rats with spinal cord injury. Cytotherapy 2017;19(7):839–48.
[11] Shiraishi Y, Kimura A, Kimura H, Ohmori T, Takahashi M, Takeshita K. Deletion of inflammasome adaptor protein ASC enhances functional recovery after spinal cord injury in mice. J Orthop Sci 2021;26(3):487–93.
[12] Jeong SK, Choi I, Jeon SR. Current status and future strategies to treat spinal cord injury with adult stem cells. Journal of Korean Neurosurgical Society 2020;63(2):153–62.
[13] Luraghi A, Peri F, Moroni L. Electrospinning for drug delivery applications: a review. J Contr Release 2021;334:463–84.
[14] Yu D-G, Huang C. Electrospun biomolecule-based drug delivery systems. MDPI; 2023. p. 1152.
[15] Liu C, Huang Y, Pang M, Yang Y, Li S, Liu L, et al. Tissue-engineered regeneration of completely transected spinal cord using induced neural stem cells and gelatin-electrospun poly (lactide-co-glycolide)/polyethylene glycol scaffolds. PLoS One 2015;10(3):e0117709.
[16] Xu J, Xi K, Tang J, Wang J, Tang Y, Wu L, et al. Engineered living oriented electrospun fibers regulate stem cell para-secretion and differentiation to promote spinal cord repair. Adv Healthcare Mater 2023;12(9):2202785.
[17] Li J, Ji Z, Wang Y, Li T, Luo J, Li J, et al. Human adipose-derived stem cells combined with nano-hydrogel promote functional recovery after spinal cord injury in rats. Biology 2022;11(5):781.
[18] Johnson CD, D'Amato AR, Gilbert RJ. Electrospun fibers for drug delivery after spinal cord injury and the effects of drug incorporation on fiber properties. Cells Tissues Organs 2016;202(1–2):116–35.
[19] Zhang Q, Li Y, Lin ZYW, Wong KK, Lin M, Yildirimer L, et al. Electrospun polymeric micro/nanofibrous scaffolds for long-term drug release and their biomedical applications. Drug Discov Today 2017;22(9):1351–66.
[20] Rahmati M, Mills DK, Urbanska AM, Saeb MR, Venugopal JR, Ramakrishna S, et al. Electrospinning for tissue engineering applications. Prog Mater Sci 2021;117:100721.
[21] Farzamfar S, Naseri-Nosar M, Vaez A, Esmaeilpour F, Ehterami A, Sahrapeyma H, et al. Neural tissue regeneration by a gabapentin-loaded cellulose acetate/gelatin wet-electrospun scaffold. Cellulose 2018;25:1229–38.
[22] Berendika M, Domjanić Drozdek S, Odeh D, Oršolić N, Dragičević P, Sokolović M, et al. Beneficial effects of laurel (Laurus nobilis L.) and myrtle (Myrtus communis L.) extract on rat health. Molecules 2022;27(2):581.
[23] Basak SS, Candan F. Effect of Laurus nobilis L. essential oil and its main components on α-glucosidase and reactive oxygen species scavenging activity. Iran J Pharm Res (IJPR): IJPR 2013;12(2):367.
[24] Lee EH, Shin JH, Kim SS, Lee H, Yang SR, Seo SR. Laurus nobilis leaf extract controls inflammation by suppressing NLRP3 inflammasome activation. J Cell Physiol 2019;234(5):6854–64.
[25] Bello AB, Kim D, Kim D, Park H, Lee S-H. Engineering and functionalization of gelatin biomaterials: from cell culture to medical applications. Tissue Eng B Rev 2020;26(2):164–80.

[26] Unal S, Arslan S, Yilmaz BK, Oktar FN, Ficai D, Ficai A, et al. Polycaprolactone/gelatin/hyaluronic acid electrospun scaffolds to mimic glioblastoma extracellular matrix. Materials 2020;13(11):2661.
[27] Calori IR, Braga G, de Jesus PdCC, Bi H, Tedesco AC. Polymer scaffolds as drug delivery systems. Eur Polym J 2020;129:109621.
[28] Dall'Acqua S, Cervellati R, Speroni E, Costa S, Guerra MC, Stella L, et al. Phytochemical composition and antioxidant activity of Laurus nobilis L. leaf infusion. J Med Food 2009;12(4):869–76.
[29] Caputo L, Nazzaro F, Souza LF, Aliberti L, De Martino L, Fratianni F, et al. Laurus nobilis: composition of essential oil and its biological activities. Molecules 2017;22(6):930.
[30] Cichon N, Saluk-Bijak J, Gorniak L, Przyslo L, Bijak M. Flavonoids as a natural enhancer of neuroplasticity—an overview of the mechanism of neurorestorative action. Antioxidants 2020;9(11):1035.
[31] Gao S, Guo X, Zhao S, Jin Y, Zhou F, Yuan P, et al. Differentiation of human adipose-derived stem cells into neuron/motoneuron-like cells for cell replacement therapy of spinal cord injury. Cell Death Dis 2019;10(8):597.
[32] Kang S-K, Shin M-J, Jung JS, Kim YG, Kim C-H. Autologous adipose tissue-derived stromal cells for treatment of spinal cord injury. Stem Cell Dev 2006;15(4):583–94.
[33] Bloom O, Herman PE, Spungen AM. Systemic inflammation in traumatic spinal cord injury. Exp Neurol 2020;325:113143.
[34] Quadri SA, Farooqui M, Ikram A, Zafar A, Khan MA, Suriya SS, et al. Recent update on basic mechanisms of spinal cord injury. Neurosurg Rev 2020;43:425–41.
[35] Ryu H-H, Lim J-H, Byeon Y-E, Park J-R, Seo M-S, Lee Y-W, et al. Functional recovery and neural differentiation after transplantation of allogenic adipose-derived stem cells in a canine model of acute spinal cord injury. J Vet Sci 2009;10(4):273–84.
[36] Silva D, Schirmer L, Pinho TS, Atallah P, Cibrão JR, Lima R, et al. Sustained release of human adipose tissue stem cell secretome from star-shaped poly (ethylene glycol) glycosaminoglycan hydrogels promotes motor improvements after complete transection in spinal cord injury rat model. Adv Healthcare Mater 2023;12(17):2202803.